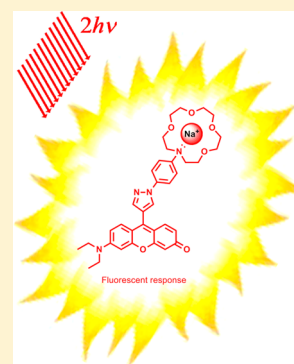


Nonlinear Optical Chemosensor for Sodium Ion Based on Rhodol Chromophore

Yevgen M. Poronik,[†] Guillaume Clermont,[‡] Mireille Blanchard-Desce,^{*,‡} and Daniel T. Gryko^{*,†}[†]Institute of Organic Chemistry of the Polish Academy of Sciences, Kasprzaka 44/52, 01-224 Warsaw, Poland[‡]Université Bordeaux, ISM (UMR5255 CNRS), F 33400 Bordeaux, France

S Supporting Information

ABSTRACT: As part of a strategy to identify good fluorescent probes based on two-photon excited fluorescence (TPEF), the sensor for sodium cation has been designed bearing a rhodol chromophore linked with an aza-crown ether. An efficient synthetic route to rhodol derivatives possessing five-membered heterocycles at position 9 and their precursors that contain xanthylium salt has been developed. The synthesis involves condensation of xanthylium salts bearing vinamidinium moiety at position 9, with phenylhydrazine derivatives as the key step. To accomplish the synthesis of derivatives bearing 1-aza-15-crown-5 and 1,10-diaza-18-crown-6, the Buchwald–Hartwig reaction has been employed in the final stage. Electronic spectra of all prepared rhodols display strong absorption in the range of 450–550 nm with well-resolved vibronic bands, which maintains its fine structure in a wide range of solvents. The most intensive two-photon absorption (2PA) band in the rhodol spectrum (165 GM), located at shorter wavelengths, matches well with the short-wavelength absorption band in the linear electronic spectrum and is most probably related to the two-photon allowed electronic transition $S_0 \rightarrow S_2$. The influence of cation binding on one- and two-photon spectroscopic properties of rhodol linked with 1-aza-15-crown-5 via the phenylpyrazole bridge has been investigated. This probe exhibits high sensitivity and good selectivity for Na^+ in CH_3CN . The mechanism involves the complexation of the Na^+ by 1-aza-15-crown-5 in the probe, which induces prominent fluorescence enhancement via quenching of electron-transfer. Interestingly, the complexation with Na^+ led to a significant increase of the 2PA band in the 750–800 nm region (corresponding to a two-photon allowed, one-photon forbidden transition) for rhodol bearing 1-aza-15-crown-5, which led to the overall enhancement of the TPEF signal (approximately an order of magnitude). Thus, a turn-on fluorescent probe for sodium ion, which does not respond to many other metal species, has been constructed.



INTRODUCTION

Fluorescence sensing is one of the most widely used detection techniques because it can provide more sensitive and selective detection with remarkable spatial and temporal patterns over other analysis methods. Discovering new fluorescent metal ion sensors has been attracting considerable attention in recent decades due to the prospect of using them in a wide range of applications including the visualization of extra- and intracellular environment for medical purposes.^{1–8} Among various ions, sodium cation is one of the most important targets because it is the most abundant monovalent metal ion in mammalian cells and a vital component of numerous enzymes.

At the same time, known fluorescent chemosensors usually based on classical linear chromophores such as cyanine and rhodamine dyes have some shortcomings since one-photon excitation mode uses the irradiation of higher energy and may cause increased risk of the damage of biological structures.^{9–11} Moreover, using the two-photon excitation mode makes it possible to achieve higher spatial resolution in the bioimaging experiments.¹² Previously reported TPEF-sensors for Na^+ were constructed on the basis of photoinduced charge transfer.¹³

Thus, the objective of this study was to design and synthesize a Na^+ -sensing system based on the following principles: (a) two-photon excitation; (b) electron-transfer quenching mech-

anism; (c) fluorescent platform possessing high Φ_f ; (d) azacrown ether previously optimized for selective sodium binding.

There are some principles of the construction of NLO chromophores imposed by the selection rules for two-photon absorption (2PA), different than for one-photon absorption (1PA), which results in particular structure of 2PA systems.^{9–11,14–16} Large 2PA cross-sections have often been associated with the extent of conjugation length (effective π -delocalization), which leads to an extended charge separation (a large π -conjugated system). Adding an electron donor D and acceptor A to the ends of a conjugated chromophore to give a D– π –A system enhances transition dipole moment as a consequence of the increase in the displacement of charge during the transition from HOMO to LUMO.^{17–24} Although chromophores with longer and easily polarizable conjugation chains tend to have higher 2PA cross-section, using bulky dye molecules in the intracellular imaging experiments is rather problematic (although this is not impossible and branched two-photon absorbing dyes have been shown to allow imaging of specific compartment within cells).²⁵ Designing novel probes

Received: August 3, 2013

Published: November 18, 2013

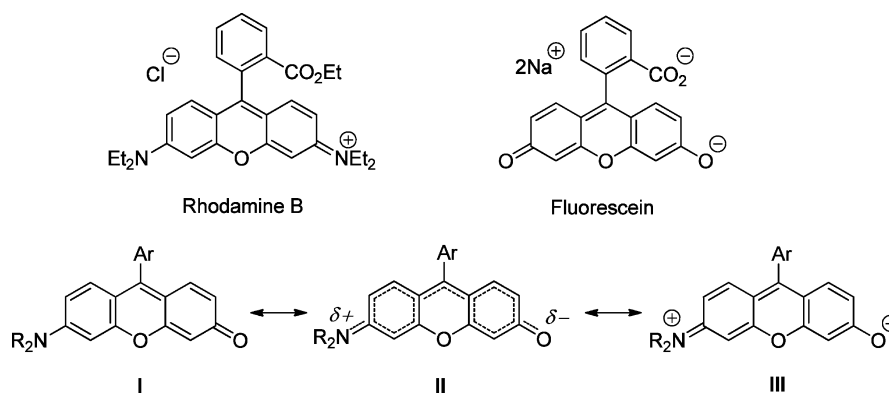


Figure 1. Resonance forms for the rhodol chromophores.

with reasonable molecular weight and combining large 2PA response in the spectral range of interest for biological imaging (700–1000 nm) with a high fluorescence quantum yield (Φ), thus yielding large two-photon brightness ($\sigma_2\Phi$), opens the way for two-photon imaging in bioenvironments by either reducing the excitation intensity (for reduced damages) or scanning more rapidly (for dynamic imaging) or alternatively to allow the detection of specific species in very low concentrations.^{9–11,26–34}

We sought to design sensing molecular system based on the well-known principle of electron-transfer quenching. Photo-induced electron transfer, which takes place from amino groups to aromatic hydrocarbons/heterocycles, causes fluorescence quenching of the latter. When the amino group strongly interacts with a given cation, electron transfer is hindered and a large enhancement of fluorescence can be expected. A fluorescent chemosensor of such type generally consists of fluorophore and receptor parts linked by nonconjugated bridge.^{35,36}

Rhodol chromophore occupies an intermediate position between the rhodamine and fluorescein. As the rhodamine chromophore contains a classical cyanine structure with the positive charge delocalized between terminal nitrogen atoms, the fluorescein chromophore possesses an oxonole structure.^{37–39} Both rhodamines and fluoresceins have an electronically symmetrical structure bridged with the oxygen atom (Figure 1).

Rhodol chromophore, displaying intrinsically high fluorescence quantum yield, possesses the merocyanine character with the electronic structure depicted by two limiting forms: neutral (I) and zwitterionic (III), and the contribution of these forms depends on the solvent polarity.^{40,41} When both resonance forms contribute equally to the ground-state structure, the molecule exhibits essentially no bond length alternation (so-called “cyanine limit”, i.e., state II). Compared with polyene molecules (traditional 2PA chromophores), merocyanine dyes may have more efficient intramolecular charge transfer (ICT) between the donor and acceptor and hence higher dipole moment (or polarization) in the ground state as well as larger 2PA cross-section for the shorter conjugated chain.²³ Overall, only a few papers on merocyanine dyes in conjunction with two-photon absorption have been published.^{42–47} Whereas rhodamine and fluorescein dyes have been widely studied, rhodol derivatives are more rarely mentioned in the literature.^{48–59} Furthermore, to the best of our knowledge, no rhodol dyes were studied in terms of their 2PA properties. Thus, we resolved to use rhodol fluorophore bearing an

additional heterocyclic unit at position 9, since (a) this position is the easiest to functionalize and (b) flexibility of the synthesis of five-membered aromatic heterocycles offers straightforward way to modify linker if necessary to fine-tune optical properties.

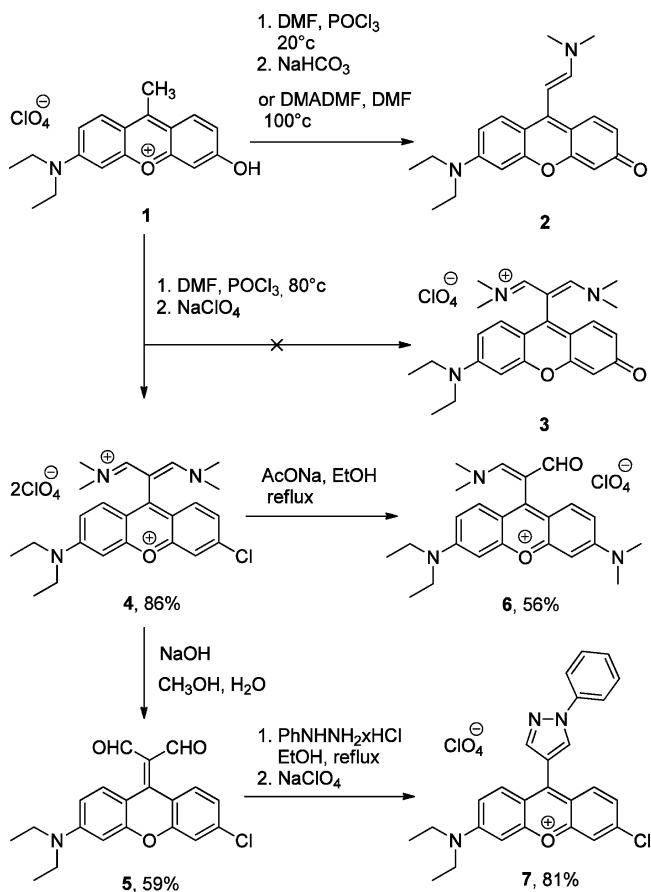
Among cation–receptor molecules, crown ethers have occupied a distinguished position due to their unique ability to strongly and selectively bind metal ions. This holds true especially for cations of two first groups of periodic table. The rationale behind the choice of 1-aza-15-crown-5 relies on the facts that 15-crown-5 is well-known to be optimized for sodium binding^{60–62} and the presence of amine makes it possible to benefit from fluorescence modulation via photoinduced electron-transfer.

RESULTS AND DISCUSSION

3-Diethylamino-6-hydroxy-substituted xanthylum salt **1**⁶³ was chosen as the key substrate for the synthesis of the rhodol-based chemosensor. In the first attempt, compound **1** was treated with the Vilsmeier reagent. It appeared that at room temperature salt **1** reacted with 1 equiv of the Vilsmeier reagent to form enamine **2** (according to ESI MS, signal 337.2). At the same time, at the higher temperature (80 °C) enamine **2** underwent the attack of the second equivalent of the Vilsmeier reagent to form vinamidinium derivative. The ¹H and ¹³C NMR spectra of the latter showed a set of signals typical of 3,6-disubstituted xanthylum salts along with the signals corresponding with the vinamidinium moiety (see the Supporting Information); however, the mass spectrum (ESI) of that vinamidinium salt showed an intensive peak with mass 205.6. It seemed that under the conditions of the Vilsmeier reaction the hydroxyl group at position 6 is substituted with the chlorine atom to form disalt with the mass of the dication 411.2. The high-resolution mass spectrum confirmed the chemical formula of the compound **4** (Scheme 1). Attempts to substitute the chlorine by the oxygen atom were not successful: treating compound **4** with either sodium hydroxide or sodium carbonate for a short period of time gave rise to the hydrolysis of vinamidinium chromophore to form dialdehyde **5**. Performing the reaction for a longer period of time led to the decomposition of the product. In the case of using sodium acetate as an *O*-nucleophile, the dimethyliminium fragment hydrolyses into the formyl group, and subsequently the chlorine atom is substituted by the dimethylamino group, so that the salt **4** rearranges into rhodamine dye **6** (Scheme 1).

Dialdehyde **5** easily formed pyrazole **7** by the condensation with the phenylhydrazine hydrochloride. Attempts to replace the chlorine atom with the hydroxyl group in the pyrazole **7**

Scheme 1



also failed. Upon addition of either sodium hydroxide or sodium carbonate into the ethanol solution of pyrazole 7, the latter immediately decolorized. After heating for several hours no conversion was observed, while the acidification of the reaction mixture brought back the initial color. We hypothesize that the xanthylium system undergoes the addition of the hydroxide anion at the position 9 to form the neutral intermediate which is much less reactive toward the nucleophiles (Figure 2).

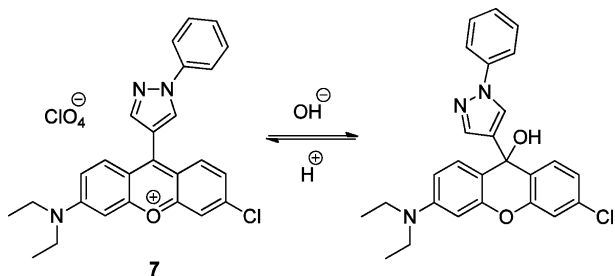
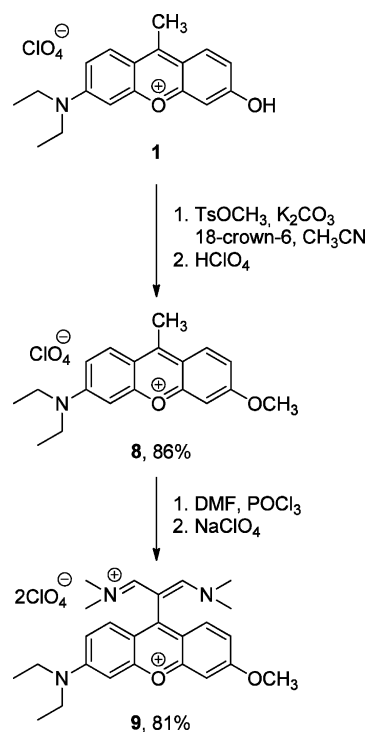


Figure 2. Addition of the hydroxide anion to the xanthylium salt 7.

To avoid the substitution with the chlorine atom we switched to *O*-protected xanthylium salts. Compound 1 was alkylated with methyl 4-toluenesulfonate according to the known procedure.⁶³ Methoxyxanthylium salt 8 was transformed into vinamidinium derivative 9 following the strategy described for dye 1 (Scheme 2).

Vinamidinium salt 9 was hydrolyzed into dialdehyde 10 in the same manner as in the case of chloro derivative 4.

Scheme 2



Compound 10 was subsequently reacted with phenylhydrazine hydrochloride to give pyrazole 11a serving as the model rhodol (Scheme 3).

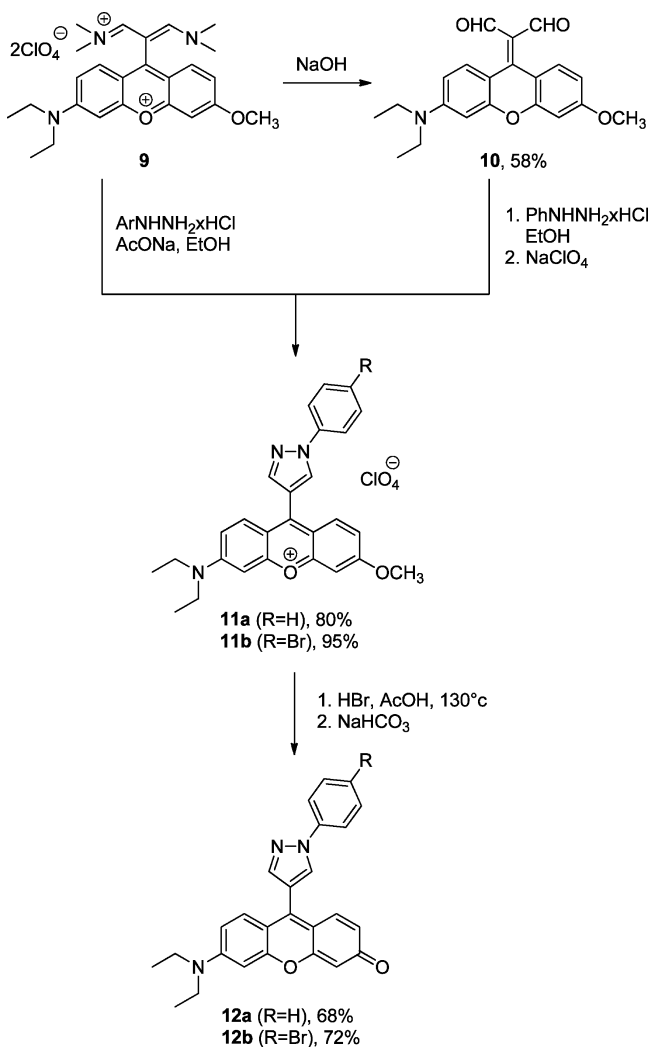
Meanwhile, we examined the reactivity of the vinamidinium chromophore toward 1,2-binnucleophiles as a latent form of malonaldehyde functionality with dimethylamine leaving groups. It appeared that disalt 9 in the presence of sodium acetate easily reacted with phenylhydrazine hydrochloride to afford *N*-phenylpyrazole 11a in high yield. Subsequently, the methoxy group was cleaved with the mixture of hydrobromic and acetic acids to give rhodol 12a. Rhodol derivative bearing bromoaryl functionality (12b) was synthesized in the similar manner (Scheme 3).

It is worth noting that, prior to our study, rhodols substituted with heterocycles at the central position were mentioned only in one patent in which the rhodol derivatives were synthesized by another, more complicated method.⁶⁴ A similar method for the introduction of heterocycles at the central position was used in the case of rhodamine dyes.⁶⁵

Subsequently, we proceeded to the synthesis of planned chemosensor molecules via the modification of rhodol 12b with azacrown ethers fragments possessing a high affinity for Na⁺ and K⁺ ions.^{66–68} It is known that cyclic oligo(ethyleneglycol) chains of azacrown ether molecules hinder the nitrogen atom for the *N*-arylation, thus decreasing the conversion and the reaction yield. In the literature there are several examples of Buchwald–Hartwig reductive amination of simple aromatic halides with azacrown ethers,^{69–72} which are carried out using predominantly Pd₂(dba)₃–DavePhos as the catalyst system and *t*-BuONa as a base.^{73–75}

In order to find suitable conditions for the amination of rhodol 12b with diazacrown ether 13 a set of experiments have been performed (Table 1). In the case of using SPhos as a ligand in the reductive amination no products were monitored. When DavePhos was used as a ligand (entry 4), formation of

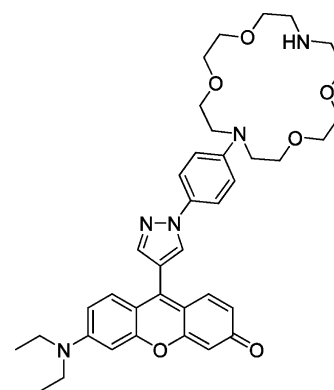
Scheme 3

Table 1. Reductive Amination of Dye 12b with Diazacrown Ether 13^a

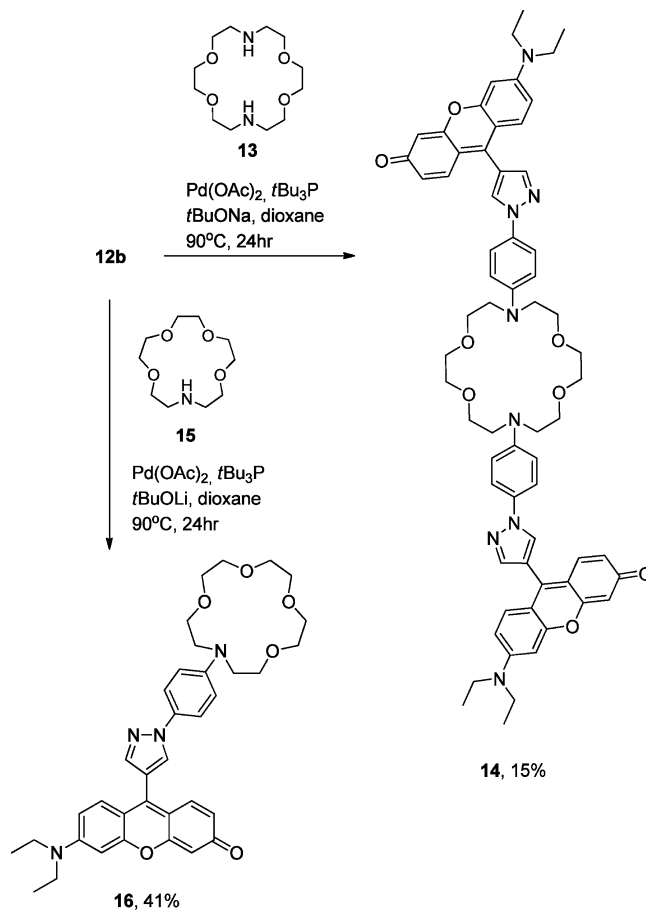
entry	catalyst/ligand	base	solvent	product (yield, %) ^b
1	Pd(OAc) ₂ /SPhos	Cs ₂ CO ₃	toluene	
2	Pd(OAc) ₂ /SPhos	<i>t</i> -BuONa	dioxane	
3	Pd(OAc) ₂ /SPhos	<i>t</i> -BuONa	toluene	
4	Pd(OAc) ₂ / DavePhos	<i>t</i> -BuONa	toluene	monocoupling (2)
5	Pd(OAc) ₂ / DavePhos	<i>t</i> -BuONa	dioxane	
6	Pd ₂ dba ₃ /DavePhos	<i>t</i> -BuONa	toluene	monocoupling (traces)
7	Pd(OAc) ₂ / DavePhos	Cs ₂ CO ₃	toluene	
8	Pd ₂ dba ₃ /DavePhos	<i>t</i> -BuONa	dioxane	
9	Pd(OAc) ₂ / <i>t</i> -Bu ₃ P	<i>t</i> -BuONa	dioxane	14 (15)

^aThe experiments were performed at 100 °C for 24 h. ^bYield of isolated products.

the new compound with low conversion was observed, which after isolation (trace amount) according to the mass spectrum was identified as the product of the monoamination (Figure 3). Nevertheless, the experiment with the catalytic system Pd(OAc)₂/*t*-Bu₃P gave rise to the formation of rhodol **14** in 15% yield (Scheme 4).

Figure 3. Product of the reductive monoamination of rhodol **12b**.

Scheme 4



Rhodol **16** was synthesized in 41% yield, analogously to dye **14** using *t*-BuOLi as base (Scheme 4).

Optical Properties. Xanthylium dyes substituted with vinamidinium chromophore (**4**, **9**) in their absorption spectra show two pronounced absorption bands: the short-wavelength one localized within vinamidinium chromophore system and the long-wavelength localized within the xanthylium chromophore. In the case of the methoxy derivative **9**, the long-wavelength band is more intense due to its more electron-symmetrical structure (Table 2, Figure 4). The product of rearrangement **6** can be considered as the electron analogue of rhodamine B substituted with a diethylaminoacroleine system. In its electronic spectrum, dye **6** exhibits a strong, narrow rhodamine-like absorption band and the Stokes shift also is

Table 2. Optical Properties of Dyes Synthesized

compd	solvent	λ_{abs} (nm)	$\epsilon \cdot 10^{-3}$ ($\text{M}^{-1} \text{cm}^{-1}$)	ΔS (cm^{-1})	λ_{em} (nm)	Φ (%)
4	CH ₃ CN	556	17	260	564	0.77
		514	21			
		307	34			
5	CH ₃ CN	569	15		nd ^a	
		479	20			
6	C ₂ H ₅ OH	560	95	600	580	28
7	CH ₃ CN	536	22	140	540	2.8
		502	26			
		408	12			
9	CH ₃ CN	549	31	900	577	0.42
		512	32			
		305	36			
10	CH ₃ CN	543	16		nd ^a	
		477	29			
11a	CH ₃ CN	528	35	1500	574	0.70
		498	31			
11b	CH ₃ CN	380	14	1600	577	0.60
		527	43			
		498	39			
12a	C ₂ H ₅ OH	528	81	800	551	74
		362	12			
	CH ₂ Cl ₂	528	50	760	550	66
		494	40			
	DMSO	352	9.6	1000	561	85
532		49				
498		36				
12b	C ₂ H ₅ OH	357	9.0	800	552	70
		529	73			
		495	31			
14	DMSO	360	11	1000	561	3.0
		532	98			
		497	77			
16	CH ₃ CN	524	53	1000	552	2.0 (10) ^b
		490	42			
		297	34			

^aFluorescence was not measured due to low S/N ratio. ^bIn the presence of the excess of NaClO₄.

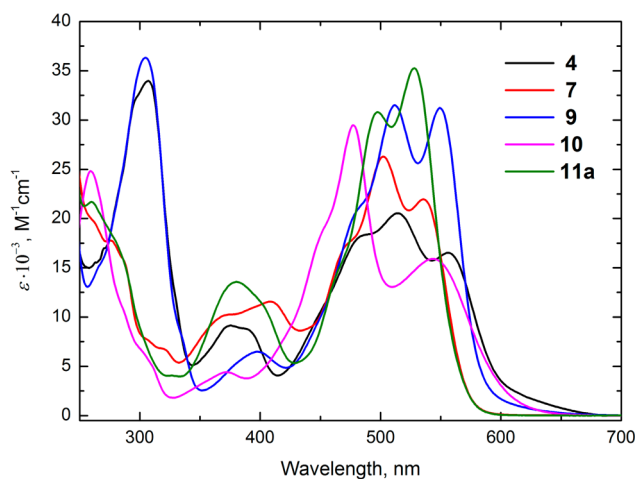


Figure 4. One-photon absorption spectra of dyes 4, 7, 9, 10, and 11a in CH₃CN.

typical of rhodamines, although fluorescent quantum yield is lower compared with rhodamine B (Table 2, Figure 4).⁷⁶

Electronic spectra of all prepared rhodols display strong absorption in the range of 450–550 nm with a well-resolved vibronic structure, which maintains its fine structure in a wide range of solvents as well as subtle absorption bands around 400 nm (Figure 5, Table 2). Examination of the linear absorption

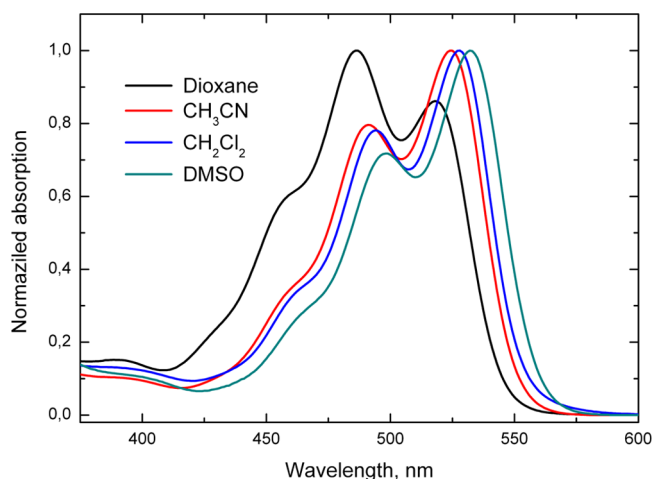


Figure 5. Normalized absorption spectra of rhodol 12a in DMSO, CH₃CN, CH₂Cl₂, and 1,4-dioxane.

spectra of rhodols reveals some regularities within the absorption bands. Analysis of solvent effects can be interpreted according to the Franck–Condon principle, the smaller bond length alternation (BLA) in the polymethine chain in the ground state, and the smaller bond lengths change in the excited state. Consequently, absorption spectra of dyes possessing electron-symmetrical structure should exhibit strong 0–0 bands at the expense of vibronic transitions.^{77,78}

Increasing solvent polarity tends to increase the contribution of the charge-separated limiting forms to the electronic ground state and thus increased π -charge density alternation. Similar to the report⁷⁷ for the DMSO model, rhodol 12a demonstrated the lowest intensity ratio between 0–1 and 0–0 subbands ($I_{0-1}/I_{0-0} = 0.72$), whereas in 1,4-dioxane the 0–1 subband is more intensive compared with the 0–0 subband ($I_{0-1}/I_{0-0} = 1.16$). Thus, the solvatochromic effect is indicated by the change of the intensity of vibronic transition and the small shift of the absorption maxima (Figure 5).

Rhodol 12a displays strong fluorescence properties in both nonpolar (CH₂Cl₂), polar aprotic (DMSO), and protic (EtOH) solvents, with fluorescent quantum yield reaches 66%, 74%, and 85%, respectively.

The optical properties of the rhodol chromophore modified with the azacrown ether 16 are similar to the model dye 12a (Table 2, Figure 1 in the Supporting Information). The only difference is that the rhodol 16 has much weaker fluorescent ability. Quenching the fluorescence occurs due to the photoinduced electron transfer (PET) from the nitrogen atom of the azacrown ether to the HOMO of the rhodol chromophore.

The absorption properties of diazacrown ether-modified rhodol 14 are somewhat different compared with model dye 12a (Figure 2, Supporting Information). Though the addition of the diazacrown ether should not affect the absorption properties, the electronic spectrum in acetonitrile displays well

Table 3. Two-Photon Absorption of Rhodol 12a in DMSO, C₂H₅OH, and CH₂Cl₂

solvent	$2\lambda_{\text{OPA}}^{\text{max}}$ (nm)	$\lambda_{\text{TPA}}^{\text{max1}}$ (nm)	$\sigma_2^{\text{max1}\Phi}$ (GM)	σ_2^{max1} (GM)	$\lambda_{\text{TPA}}^{\text{max2}}$ (nm)	$\sigma_2^{\text{max2}\Phi}$ (GM)	σ_2^{max2} (GM)	$\lambda_{\text{TPA}}^{\text{max3}}$ (nm)	$\sigma_2^{\text{max3}\Phi}$ (GM)	σ_2^{max3} (GM)
CH ₂ Cl ₂	1056	1060	20	30	920	51.7	78.7	790	109	165
C ₂ H ₅ OH	1056	1060	35	47	980	68	92	820	85	115
DMSO	1064	nd ^a			≥920	≥37.6	≥44.1	820	100	117

^a2PA was not measured for 1000–1200 nm range.

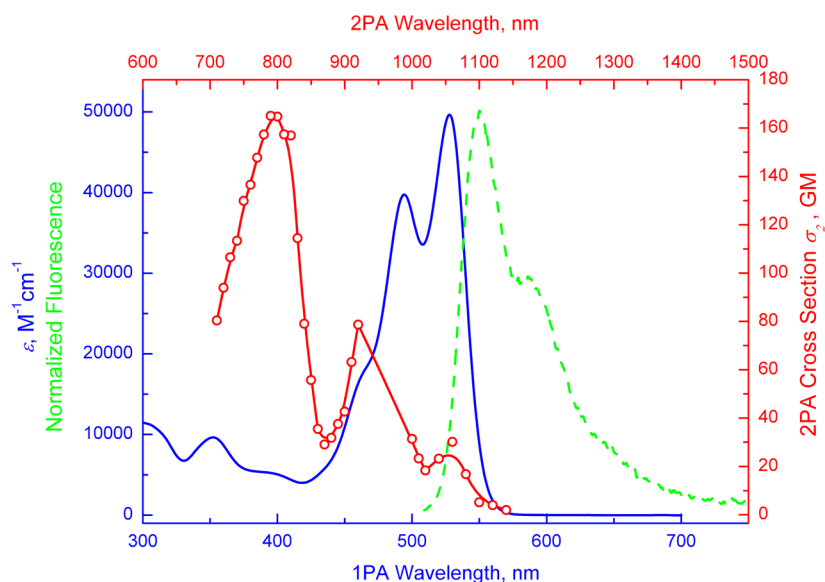


Figure 6. 1PA (blue), 2PA (red), and normalized fluorescence spectra (green) of dye 12a in CH₂Cl₂.

resolved 0–1 and 0–0 subbands with the commensurate intensity. We assume that in acetonitrile solution two rhodol chromophores can approach each other, which can lead to the interaction between the electronic levels of two chromophores.

The two-photon absorption spectrum of model rhodol 12a in methylene chloride consists of three bands. The weakest long-wavelength band has the absorption maximum at 1056 nm, which corresponds with the 0–0 subband in the 1PA spectrum, typical of D–π–A chromophores.^{14,15,19–21,49} For better comparison, the 2PA spectrum is shown on the same graph as 1PA by multiplying the wavelength scale by 2, with separate axes (Table 3, Figure 6). Moreover, 2PA spectrum of the rhodol molecule shows weak absorption band (25 GM) somewhat hypsochromically shifted as compared with the maximum of the S₀→S₁ transition. The latter can probably be attributed to the vibrational coupling between the first excited state S₁ and its vibrational modes.⁴⁹ The most intensive 2PA band in rhodol spectrum (165 GM), located at shorter wavelengths, matches well with the subtle short-wavelength absorption band in the linear electronic spectrum and is most probably related to the two-photon allowed electronic transition S₀→S₂. 2PA cross-section is only slightly lower in solvents mimicking intracellular environment (EtOH) and cell membrane (DMSO) (Table 3). While the value of σ_2 of the rhodol chromophore is rather moderate, two-photon brightness ($\sigma_2^{\text{max}\Phi}$) of this dye is sufficient for two-photon excited fluorescence microscopy purposes.^{79,80}

Metal Ion Binding Properties. Dye molecule 16 which featured crown ether moieties demonstrates properties of selective two-photon fluorescent probe for alkali metal ions sensing. When alkali metal ion is complexed with crown ether the free electron pair of the nitrogen atom is partly shifted

toward metal ion, thus blocking PET and consequently giving rise to an increase in fluorescence. While compound 14 showed no changes in fluorescence properties upon addition of Na⁺, K⁺, Li⁺, and Mg²⁺-containing salts, compound 16 demonstrated marked response upon addition of Na⁺, weak response for K⁺ and no response upon addition of Mg²⁺ or Li⁺ containing salts. (Figure 7). The reason why compound 14 failed to show a response upon the addition of metal ions is probably because of only partial quenching of electron transfer upon complexation. As reported by Mateeva et al., 1,10-diaza-18-crown-6 derivatives show more pronounced fluorescence changes in the presence of divalent cations.^{13c} The presence of

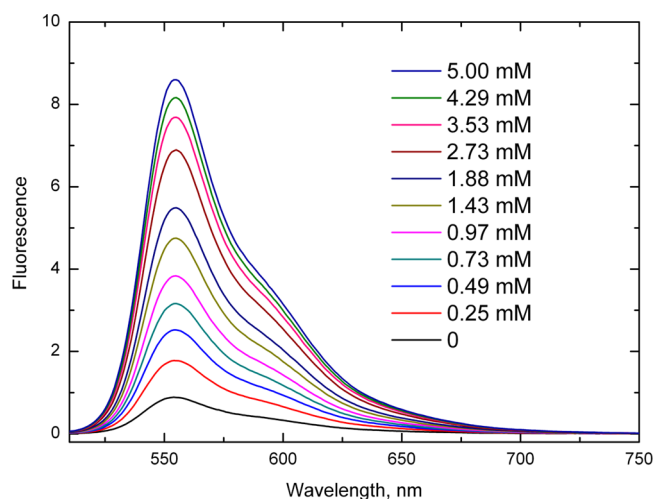


Figure 7. Emission spectra of dye 16 at different [Na⁺] in CH₃CN.

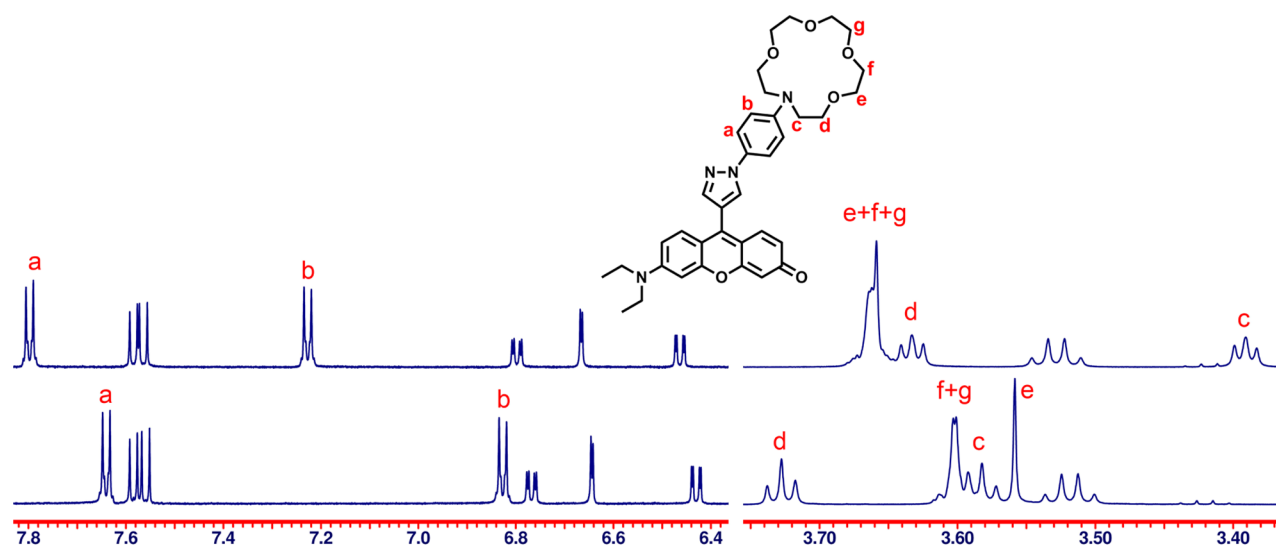


Figure 8. ^1H NMR spectra of free rhodol **16** (below) and the complex of **16** with Na^+ (above) in CD_3CN .

Table 4. 2PA Properties of Dyes **14** (in DMSO) and **16** (in CH_3CN) upon Complexation with Metal Cations

compd	$2\lambda_{\text{OPA}}^{\text{max}}$ (nm)	$\lambda_{\text{TPA}}^{\text{max1}}$ (GM)	$\sigma_2^{\text{max1}} \cdot \Phi$ (GM)	σ_2^{max1} (GM)	$\lambda_{\text{TPA}}^{\text{max2}}$ (nm)	$\sigma_2^{\text{max2}} \cdot \Phi$ (GM)	σ_2^{max2} (GM)	$\lambda_{\text{TPA}}^{\text{max3}}$ (GM)	$\sigma_2^{\text{max3}} \cdot \Phi$ (GM)	σ_2^{max3} (GM)
14	1064	nd ^a			nd ^a			790	5.8	193
14 + KPF_6	1050	nd ^a			nd ^a			790	5.5	267
16	1048	1080	2.2	110	970	1.7	86	770	1.4	72
16 + NaClO_4	1050	1060	6.3	63	970	21.6	216	770	18	176
16 + LiClO_4	1050	1080	3.1	102	970	3.7	125	820	4.3	144
16 + $\text{Mg}(\text{ClO}_4)_2$	1048	1080	2.9	147	970	1.7	86	820	3.0	151
16 + KPF_6	1046	1060	2.8	138	970	7.1	353	820	6.7	335

^aTPA was not measured in this spectral range.

two rhodol moieties can also interfere with typical mechanism of fluorescence modulating.

The formation of the sodium ion complex with dye **16** is also demonstrated by NMR spectroscopy. The addition of sodium perchlorate into the solution of rhodol **16** in CD_3CN gives rise to the shift of the crown ether moiety peaks along with the peaks of phenyl ring adjacent to the crown ether (Figure 8). Peaks assignment was performed on the basis of HSQC and HMBC experiments.

The addition of the crown ether fragment (dye **16**) also affects the nonlinear properties of the rhodol chromophore (Table 4). Compared with the model dye **12a** the addition of monoazacrown ether fragment decreases the short-wavelength absorption band and increases the intensity of the bands corresponding with the one-photon allowed transition in its 2PA spectrum (Figure 9, Table 4). At the same time, the presence of metal salts affects both 2PA properties and the fluorescence ability. Furthermore, the 2PA spectrum displays different effects for the low energy and high energy bands. The presence of Li^+ ion causes an almost 2-fold increase of short-wavelength band, a somewhat increase of the band located at 970 nm and hardly influences the long-wavelength band. Compared with free derivative **16** the fluorescence does not change. The presence of Mg^{2+} ion has no influence on the band located at 970 nm but increases the intensity of low energy and high energy bands with no influence on the fluorescence. The addition of K^+ ion into the solution of **16** gives rise to a significant increase of the second (970 nm) and the high energy

(820 nm) bands; however, there are no changes in the fluorescence properties (Figures 9 and 10).

The addition of Na^+ ion decreased the intensity of the low energy band however the intensity of the second and the high energy bands are significantly increased. The fluorescence ability in the presence of sodium ion is also increased. It appears that the second band located at 970 nm (which is both one and two-photon allowed) is more selective and sensitive to the presence of Na^+ (2PA increases by more than 2) following the trend of fluorescence. Hence the TPEF signal is increased by more than 1 order of magnitude (Figures 9 and 10, Table 4), demonstrating the ability of new dye **16** to act as sensitive two-photon probe for sensing the presence of Na^+ ion in acetonitrile. Yet, for application of such rhodol-based chemosensors in aqueous media, modifications should be made to further increase their two-photon absorption cross-section as well as their solubility in aqueous environments.

CONCLUSIONS

The method of heterocyclization at the 9-position of the rhodol chromophore was developed. The strategy presented herein enables transformation of 4-dimethylamino-2-hydroxyacetophenone into pyrazolylrhodols in five steps (36–45% overall yields). It was shown that direct transformation of **1** into **3** cannot be successful due to concomitant chlorination resulting in chlororhodol **4**, which is not prone to further transformations.

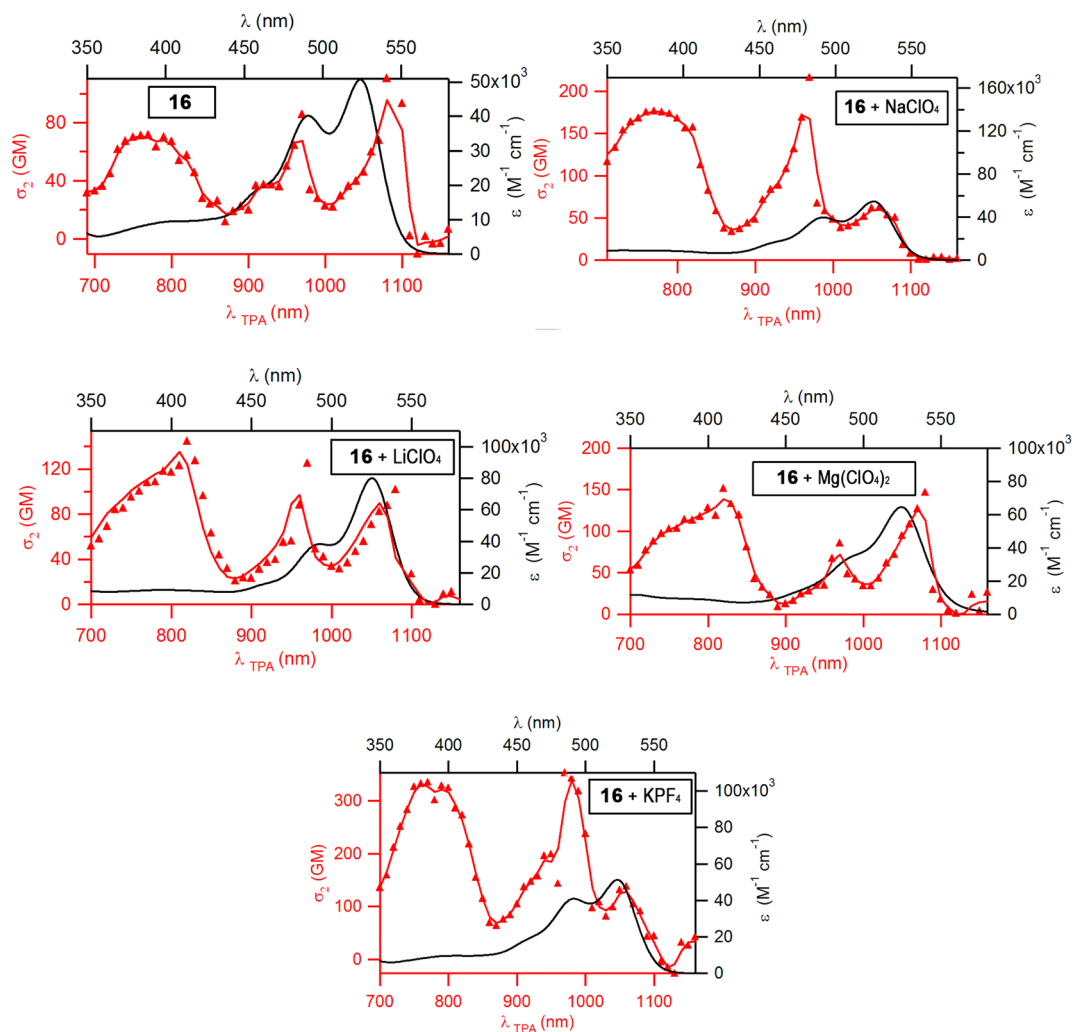


Figure 9. Two-photon properties of the dye **16** upon addition of metal salts in acetonitrile.

Linear absorption spectra of dyes synthesized consist of two bands, an intense long-wavelength one with a well-resolved vibronic structure and a weak short-wavelength one. The two-photon absorption spectrum of model rhodol consists of three bands. The weakest long-wavelength band has the absorption maximum that well corresponds with the 0–0 subband in 1PA spectrum, typical of D– π –A chromophores, somewhat hypsochromically shifted weak absorption band attributed to the vibrational coupling between S_1 state and its vibrational modes. The strongest 2PA band located at shorter wavelengths is most probably related to the two-photon allowed electronic transition $S_0 \rightarrow S_2$.

Although the addition of crown ether fragments gives rise to the almost 2-fold decrease in 2PA compared with the model rhodol, the addition of metal salts into solutions of chemosensor molecules increases the 2PA. Moreover, the rhodol-modified with monoazacrown ether demonstrates a good fluorescence response on the addition of Na^+ and weak response for K^+ , thus resulting in the significant increase of two-photon brightness for Na^+ .

EXPERIMENTAL SECTION

All chemicals were used as received unless otherwise noted. Reagent-grade CH_2Cl_2 was distilled prior to use. All reported ^1H NMR spectra were collected using 400, 500, and 600 MHz spectrometers. Chemical

shifts (δ ppm) were determined with TMS as the internal reference; J values are given in hertz. Chromatography was performed on silica gel (230–400 mesh) or neutral aluminum oxide (70–230 mesh). Preparative size-exclusion chromatography (SEC) was carried out using BioRad Bio-Beads SX-1. The mass spectra were obtained via electrospray ionization (ESI-MS). For the complexation experiments 10^{-3} M solutions of LiClO_4 , NaClO_4 , $\text{Mg}(\text{ClO}_4)_2$, and KPF_6 in acetonitrile were used. All photophysical studies have been performed with freshly prepared air-equilibrated solutions at room temperature (298 K). TPEF cross sections of 10^{-4} M solutions were measured relative to fluorescein in 0.01 M aqueous NaOH for 700–800 nm,⁸¹ using the well-established method described by Xu and Webb^{81b} and the appropriate solvent-related refractive index corrections.⁸² Reference values between 700 and 715 nm for fluorescein were taken from literature.⁸³ The quadratic dependence of the fluorescence intensity on the excitation power was checked for each sample and all wavelengths. To span the 700–980 nm range, a Nd:YLF-pumped Ti:sapphire oscillator was used generating 150 fs pulses at a 76 MHz rate. To span the 1000–1400 nm range, an OPO (PP-BBO) was added to the setup to collect and modulate the output signal of the Ti:sapphire oscillator.

3-Chloro-6-diethylamino-9-(1-dimethylamino-3-(dimethyliminio)prop-1-en-2-yl)xanthylum Perchlorate (4). Compound **1** (2.9 g, 7.6 mmol) was dissolved in 20 mL of dry DMF, and phosphorus oxychloride (4.66 g, 30 mmol, 2.8 mL) was added dropwise with stirring so that the internal temperature did not rise above 50 °C. After addition, the reaction was heated at 80 °C for 1 h. On cooling, the mixture was poured on ice and neutralized with a water solution of NaHCO_3 followed by extraction with CH_2Cl_2 and

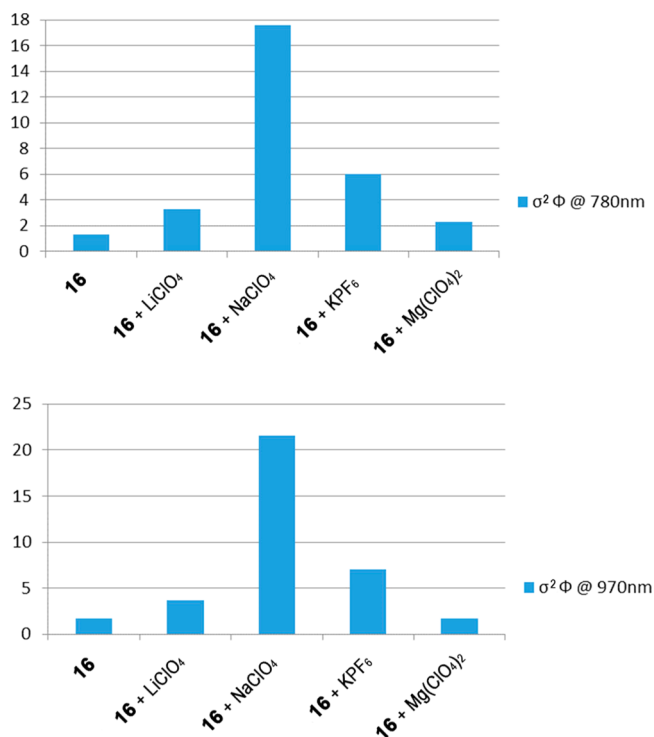


Figure 10. Bar diagram with the TPEF signal of dye **16** in the presence of salts for excitation at 780 nm (upper panel) and 970 nm (lower panel).

drying over Na₂SO₄. The solvent was evaporated, and the residue was recrystallized from ethanol to give 3.99 g (86%) of the pure product. Mp: 228–229 °C. ¹H NMR (500 MHz, DMSO-*d*₆): 8.19 (s, 2H), 8.05 (s, 1H), 7.92 (d, *J* 8.7 Hz, 1H), 7.84 (d, *J* 9.8 Hz, 1H), 7.73 (d, *J* 8.6 Hz, 1H), 7.58 (d, *J* 9.9 Hz, 1H), 7.28 (s, 1H), 3.95–3.85 (m, 4H), 3.32 (s, 6H), 2.45 (s, 6H), 1.35–1.26 (m, 6H). ¹³C NMR (125 MHz, DMSO-*d*₆): 164.6, 158.7, 157.8, 152.8, 148.9, 141.6, 132.4, 130.7, 127.3, 122.0, 121.0, 120.7, 117.9, 97.5, 91.3, 48.9, 47.1, 46.9, 40.0, 13.4, 12.4. HRMS (ESI-TOF) calcd for [C₂₄H₃₀ClN₃O]²⁺ 205.6039 [M²⁺], found 205.6042. Anal. Calcd for C₂₄H₃₀Cl₃N₃O₉ (610.87): C, 47.19; H, 4.95; N, 6.88; Cl, 17.41. Found: C, 47.28; H, 4.99; N, 6.84; Cl, 16.85. λ_{abs} (CH₃CN, $\epsilon \times 10^{-3}$): 307 (34), 514 (21), 556 (17) nm.

2-(3-Chloro-6-diethylamino-9H-xanthen-9-ylidene)-malonaldehyde (5). A solution of xanthylium salt **4** (0.61 g, 1 mmol) and NaOH (0.4 g, 10 mmol) in 20 mL of 50% mixture of CH₃OH and water was heated at reflux for 5 min. On cooling, the mixture was diluted with water and AcOH (0.75 mL) was added followed by the extraction with CH₂Cl₂ and drying over Na₂SO₄. The solvent was evaporated off, and the residue was eluted through a silica column (CH₂Cl₂–CH₃OH 14:1) to give 0.21 g (59%) of compound **5**. Mp: 146–148 °C. ¹H NMR (600 MHz, CD₃CN): 9.38 (s, 2H), 8.10 (d, *J* 8.8 Hz, 1H), 7.91 (d, *J* 9.7 Hz, 1H), 7.64 (s, 1H), 7.38 (d, *J* 8.7 Hz, 1H), 7.08 (d, *J* 9.9 Hz, 1H), 6.74 (s, 1H), 3.67 (q, *J* 7.2 Hz, 4H), 1.29 (t, *J* 7.1 Hz, 6H). ¹³C NMR (150 MHz, CD₃CN): 186.2, 159.0, 158.5, 157.5, 153.8, 140.5, 135.6, 133.2, 124.8, 119.8, 117.5, 117.1, 114.6, 95.3, 46.0, 11.9. HRMS (ESI-TOF): calcd for C₂₀H₁₈ClNO₃ 356.10480 [M + H⁺], found 356.10477. Anal. Calcd for C₂₀H₁₈ClNO₃·0.5H₂O (364.82): C, 65.84; H, 5.25; N, 3.84. Found: C, 66.11; H, 5.48; N, 4.01. λ_{abs} (CH₃CN, $\epsilon \times 10^{-3}$): 479 (20), 569 (15) nm.

3-Diethylamino-6-dimethylamino-9-(1-dimethylamino-3-oxoprop-1-en-2-yl)xanthylium Chloride (6). Xanthylium salt **4** (0.24 g, 0.5 mmol) and sodium acetate (0.05 g, 0.61 mmol) in ethanol (4 mL) were heated at reflux for 2 h. On cooling, the precipitated product was filtered and washed with ethanol to give 0.12 g (56%) of compound **6**. Mp: 235 °C. ¹H NMR (400 MHz, CD₃CN): 9.18 (s, 1H, CHO), 7.65–7.56 (m, 3H), 7.08–7.00 (m, 2H), 6.76 (d, *J* 2.8 Hz,

1H), 6.73 (d, *J* 2.4 Hz, 1H), 3.62 (q, *J* 7.2 Hz, 4H), 3.24 (s, 6H), 3.20 (br s, 3H), 2.43 (br s, 3H), 1.26 (t, *J* 7.2 Hz, 6H). ¹³C NMR (100 MHz, CD₃CN): 187.3, 162.0, 158.6, 158.3, 158.2, 156.8, 156.3, 133.1, 132.6, 115.7, 115.5, 115.1, 114.9, 105.0, 97.0, 96.8, 47.4, 46.6, 41.2, 40.2, 12.8. HRMS (ESI-TOF): calcd for [C₂₄H₃₀N₃O₂]⁺ 392.2338 [M⁺], found 392.2329. λ_{abs} (C₂H₅OH, $\epsilon \times 10^{-3}$): 560 (95) nm.

3-Chloro-6-diethylamino-9-(1-phenyl-1H-pyrazol-4-yl)-xanthylium Perchlorate (7). Dialdehyde **5** (71 mg, 0.2 mmol) and phenylhydrazine hydrochloride (30 mg, 0.2 mmol) in ethanol (4 mL) were heated at reflux for 15 min. On cooling, a solution of NaClO₄ × H₂O (56 mg, 0.4 mmol) in ethanol (4 mL) was added to the reaction mixture. The precipitate was filtered and washed with ethanol to give 85 mg (81%) of the product. Mp: 138–139 °C. ¹H NMR (400 MHz, DMSO-*d*₆): 9.28 (s, 1H), 8.32 (s, 1H), 8.19 (d, *J* 9.2 Hz, 1H), 8.1–8.0 (m, 4H), 7.69 (dd, *J* 8.8 Hz *J* 2.0 Hz, 1H), 7.62 (t, *J* 8.0 Hz, 2H), 7.54 (dd, *J* 10.0 Hz *J* 2.0 Hz, 1H), 7.46 (t, *J* 7.6 Hz, 1H), 7.24 (d, *J* 2.0 Hz, 1H), 3.87 (br s, 4H), 1.4–1.2 (m, 6H, CH₃). ¹³C NMR (100 MHz, DMSO-*d*₆): 158.6, 158.0, 153.6, 148.4, 142.9, 141.1, 138.9, 133.7, 131.5, 129.8, 127.7, 126.7, 119.3, 119.2, 119.1, 118.0, 117.5, 113.7, 96.9, 46.8, 46.6, 13.4, 12.4. HRMS (ESI-TOF): calcd for [C₂₆H₂₃ClN₃O]⁺ 428.15242 [M⁺], found 428.15258. λ_{abs} (CH₃CN, $\epsilon \times 10^{-3}$): 408 (12), 502 (26), 536 (22) nm.

3-Diethylamino-9-(1-dimethylamino-3-(dimethyliminio)-prop-1-en-2-yl)-6-methoxyxanthylium Dipерchlorate (9). Compound **9** was prepared identically to **4**. Yield: 81%. Mp: 216 °C. ¹H NMR (400 MHz, CD₂Cl₂): 8.14 (s, 2H), 7.95 (d, *J* 9.6 Hz, 1H), 7.90 (d, *J* 8.8 Hz, 1H), 7.37 (dd, *J* 9.6 Hz *J* 2.4 Hz, 1H), 7.28 (dd, *J* 8.8 Hz *J* 2.4 Hz, 1H), 7.24 (d, *J* 2.4 Hz, 1H), 6.95 (d, *J* 2.4 Hz, 1H), 4.06 (s, 3H), 3.85–3.70 (m, 4H), 3.40 (s, 6H), 2.48 (s, 6H), 1.45–1.30 (m, 6H). ¹³C NMR (100 MHz, CD₂Cl₂): 168.9, 165.4, 158.4, 158.0, 156.1, 132.7, 131.3, 119.4, 118.2, 116.9, 101.4, 97.4, 92.4, 57.2, 49.8, 47.5, 47.3, 39.8, 13.2, 12.1. HRMS (ESI-TOF): calcd for [C₂₅H₃₃N₃O₂]²⁺ 203.6287 [M²⁺], found 203.6291. Anal. Calcd for C₂₅H₃₃Cl₂N₃O₁₀ (606.45): C, 49.51; H, 5.48; N, 6.93; Cl, 11.69. Found: C, 49.44; H, 5.54; N, 6.87; Cl, 11.54. λ_{abs} (CH₃CN, $\epsilon \times 10^{-3}$): 305 (36), 512 (32), 549 (31) nm.

2-(3-Diethylamino-6-methoxy-9H-xanthen-9-ylidene)-malonaldehyde (10). Compound **10** was prepared identically to **5**. Yield: 58%. Mp: 198 °C (dec). ¹H NMR (400 MHz, CDCl₃): 9.39 (s, 2H), 8.12 (d, *J* 9.2 Hz, 1H), 8.03 (d, *J* 9.6 Hz, 1H), 7.03 (dd, *J* 9.2 Hz *J* 2.4 Hz, 1H), 6.96 (d, *J* 2.8 Hz, 1H), 6.92 (dd, *J* 9.6 Hz *J* 2.4 Hz, 1H), 6.62 (d, *J* 2.8 Hz, 1H), 3.97 (s, 3H), 3.60 (q, *J* 7.2 Hz, 4H), 1.33 (t, *J* 7.2 Hz, 6H). ¹³C NMR (100 MHz, CDCl₃): 187.4, 167.0, 161.6, 159.0, 156.9, 156.4, 135.8, 134.2, 116.2, 115.6, 115.2, 114.9, 113.6, 99.4, 95.1, 56.3, 46.0, 12.8. HRMS (ESI-TOF): calcd for C₂₁H₂₂NO₄ 352.1549 [M + H⁺], found 352.1551. Anal. Calcd for C₂₁H₂₂NO₄·0.5H₂O (360.40): C, 69.98; H, 6.15; N, 3.89. Found: C, 70.17; H, 6.14; N, 4.04. λ_{abs} (CH₃CN, $\epsilon \times 10^{-3}$): 477 (29), 543 (16) nm.

3-Diethylamino-6-methoxy-9-(1-phenyl-1H-pyrazol-4-yl)-xanthylium Perchlorate (11a). Vinamidinium salt **9** (0.82 g, 1.34 mmol), phenylhydrazine hydrochloride (0.27 g, 1.9 mmol), and sodium acetate (0.33 g, 4 mmol) in ethanol (20 mL) were heated at reflux for 2 h. On cooling, the product precipitated was filtered and washed with ethanol to give 0.56 g (80%) of the pure product. Mp: 126–127 °C. ¹H NMR (400 MHz, DMSO-*d*₆): 9.27 (s, 1H), 8.31 (s, 1H), 8.13 (d, *J* 9.2 Hz, 1H), 8.08–8.00 (m, 3H), 7.65–7.57 (m, 2H), 7.48–7.40 (m, 3H), 7.28 (dd, *J* 9.2 Hz *J* 2.4 Hz, 1H), 7.16 (d, *J* 2.0 Hz, 1H), 4.06 (s, 3H), 3.9–3.7 (m, 4H), 1.27 (br s, 6H). ¹³C NMR (100 MHz, DMSO-*d*₆): 167.0, 158.5, 156.9, 156.3, 149.8, 142.8, 138.9, 133.2, 131.8, 131.3, 129.8, 127.6, 119.2, 117.5, 116.4, 115.3, 114.4, 113.9, 100.6, 96.3, 57.0, 46.2, 46.0, 13.2, 12.1. HRMS (ESI-TOF): calcd for [C₂₇H₂₆N₃O₂]⁺ 424.20195 [M⁺], found 424.20355. λ_{abs} (CH₃CN, $\epsilon \times 10^{-3}$): 380 (14), 498 (31), 528 (35) nm.

Method for the Preparation of Compound 11a from Compound 10. Dialdehyde **10** (175 mg, 0.5 mmol) and phenylhydrazine hydrochloride (75 mg, 0.52 mmol) in ethanol (7 mL) were heated at reflux for 15 min. On cooling, a solution of NaClO₄·H₂O (140 mg, 1.0 mmol) in ethanol (5 mL) was added to the reaction mixture. The precipitate was filtered and washed with ethanol to give

220 mg (85%) of the product. Spectral data are identical to the previous experiment.

9-(1-(4-Bromophenyl)-1H-pyrazol-4-yl)-3-diethylamino-6-methoxyxanthylum Perchlorate (11b). Compound 11b was prepared identically to 11a. Yield: 95%. Mp: 258 °C (dec). ¹H NMR (500 MHz, DMSO-*d*₆): 9.26 (s, 1H), 8.33 (s, 1H), 8.12 (d, J 9.0 Hz, 1H), 8.03 (d, J 9.8 Hz, 1H), 8.00 (d, J 8.9 Hz, 2H), 7.82 (d, J 8.9 Hz, 2H), 7.45–7.40 (m, 2H), 7.28 (dd, J 9.2 Hz J 2.6 Hz, 1H), 7.17 (d, J 2.4 Hz, 1H), 4.06 (s, 3H), 3.83–3.77 (m, 4H), 1.28 (br s, 6H). ¹³C NMR (125 MHz, DMSO-*d*₆): 167.5, 159.0, 157.4, 156.8, 150.1, 143.5, 138.6, 133.6, 133.0, 132.2, 131.8, 121.6, 120.5, 117.9, 116.8, 115.9, 114.8, 114.6, 101.1, 96.8, 57.5, 46.7, 46.5, 13.6, 12.6. HRMS (ESI-TOF): calcd for [C₂₇H₂₅BrN₃O₂]⁺ 502.1130 [M⁺], found 502.1127. Anal. Calcd for C₂₇H₂₅BrClN₃O₆ (602.86): C, 53.79; H, 4.18; N, 6.97. Found: C, 53.76; H, 4.32; N, 6.97. λ_{abs} (CH₃CN, $\epsilon \times 10^{-3}$): 382 (19), 498 (39), 527 (43) nm.

6-Diethylamino-9-(1-phenyl-1H-pyrazol-4-yl)-3H-xanthen-3-one (12a). Compound 11a (0.26 g, 0.5 mmol) was dissolved in a mixture of 5 mL of glacial acetic acid and 3 mL of 48% hydrobromic acid and heated at 130 °C for 10 h. On cooling, the reaction mixture was diluted with water and neutralized with a solution of NaHCO₃ followed by extraction with CH₂Cl₂ and drying over MgSO₄. The solvent was evaporated, and the residue was eluted through an Al₂O₃ column (CH₂Cl₂–CH₃OH 96:4) to give 0.14 g (68%) of rhodol 11a. Mp: 137–138 °C. ¹H NMR (400 MHz, CDCl₃): 8.20 (s, 1H), 7.90 (s, 1H), 7.82–7.78 (m, 2H), 7.57–7.43 (m, 4H), 7.39 (tt, J 7.6 Hz J 1.6 Hz, 1H), 6.68–6.62 (m, 2H), 6.60 (d, J 2.8 Hz, 1H), 6.48 (br s, 1H), 3.50 (q, J 7.2 Hz, 4H), 1.27 (t, J 7.2 Hz, 6H). ¹³C NMR (100 MHz, CDCl₃): 159.0, 156.1, 152.6, 142.0, 139.6, 130.4, 129.9, 128.1, 128.0, 127.6, 119.5, 115.4, 115.3, 110.6, 110.4, 105.4, 96.9, 45.3, 12.7. HRMS (ESI-TOF): calcd for C₂₆H₂₃N₃O₂ 410.18630 [M + H⁺], found 410.18786. Anal. Calcd for C₂₆H₂₃N₃O₂·H₂O (427.50): C, 73.05; H, 5.89; N, 9.83. Found: C, 72.87; H, 5.70; N, 9.85. λ_{abs} (C₂H₅OH, $\epsilon \times 10^{-3}$): 362 (12), 494 (36), 527 (87) nm.

9-(1-(4-Bromophenyl)-1H-pyrazol-4-yl)-6-diethylamino-3H-xanthen-3-one (12b). Compound 12b was prepared identically to 12a. Yield: 72%. Mp: 256–257 °C. ¹H NMR (400 MHz, CDCl₃): 8.14 (s, 1H), 7.89 (s, 1H), 7.72–7.62 (m, 4H), 7.45–7.38 (m, 2H), 6.65–6.58 (m, 3H), 6.43 (d, J 2.0 Hz, 1H), 3.49 (q, J 7.2 Hz, 4H), 1.27 (t, J 7.2 Hz, 6H). ¹³C NMR (100 MHz, CDCl₃): 185.3, 182.9, 159.0, 155.9, 152.4, 142.3, 141.0, 138.6, 132.9, 130.3, 129.6, 128.5, 127.8, 120.9, 115.9, 115.5, 110.4, 110.1, 105.6, 97.0, 45.2, 12.7. HRMS (ESI-TOF): calcd for C₂₆H₂₂BrN₃O₂ 488.0974 [M + H⁺], found 488.0971. Anal. Calcd for C₂₆H₂₂BrN₃O₂ (488.38): C, 63.94; H, 4.54; N, 8.60; Br, 16.36. Found: C, 63.87; H, 4.75; N, 8.58; Br, 16.35. λ_{abs} (C₂H₅OH, $\epsilon \times 10^{-3}$): 360 (11), 495 (31), 529 (73) nm.

9,9'-(1,1'-(4,4'-(1,4,10,13-Tetraoxa-7,16-diazacyclooctadecane-7,16-diyl)bis(4,1-phenylene))bis(1H-pyrazole-4,1-diyl))bis(6-diethylamino-3H-xanthen-3-one) (14). Rhodol 12b (0.49 g, 1 mmol), diazacrown ether 13 (0.13 g, 0.5 mmol), sodium *tert*-butoxide (0.16 g, 1.7 mmol), and palladium diacetate (9 mg, 0.04 mmol) were placed into a dried Schenk flask. The flask was capped, subsequently degassed several times, and filled with argon. Then a 0.25 M toluene solution of tri-*tert*-butylphosphine (0.13 mL, 0.032 mmol) and 7 mL of dry degassed dioxane were added to the inert atmosphere. The stirred reaction mixture was heated at 90 °C for 24 h. On cooling, the mixture was diluted with CH₂Cl₂ (30 mL), and solid material was filtered off. Solvents were evaporated off, and the residue was eluted through the silica column (CH₂Cl₂–CH₃OH 85:15). The fraction consisted of compound 14 and was evaporated. The crude product (100 mg) was purified on SEC in CHCl₃ to give 80 mg (15%) of the title compound. Mp: 174 °C. ¹H NMR (400 MHz, CDCl₃): 7.99 (s, 2H), 7.79 (s, 2H), 7.58–7.49 (m, 6H), 7.47 (d, J 10.0 Hz, 2H), 6.74 (d, J 9.2 Hz, 4H), 6.70–6.62 (m, 4H), 6.56 (d, J 2.4 Hz, 2H), 6.50 (br s, 2H), 3.74 (t, J 5.6 Hz, 8H), 3.70–3.60 (m, 16H), 3.51 (q, J 7.2 Hz, 8H), 1.27 (t, J 7.2 Hz, 12H). ¹³C NMR (100 MHz, CDCl₃): 182.9, 158.8, 156.3, 153.0, 147.6, 141.3, 130.6, 130.1, 129.3, 128.0, 126.9, 121.2, 114.7, 114.4, 112.2, 110.8, 105.1, 96.8, 71.3, 69.2, 51.8, 45.5, 12.8. HRMS (ESI-TOF): calcd for C₆₄H₆₈N₈O₈ 1077.5238 [M + H⁺], found 1077.5245. Anal. Calcd for C₆₄H₆₈N₈O₈·2H₂O (1113.30): C,

69.05; H, 6.52; N, 10.06. Found: C, 69.08; H, 6.40; N, 10.11 λ_{abs} (DMSO, $\epsilon \times 10^{-3}$): 497 (77), 532 (98) nm.

9-(1-(4-(1,4,7,10-Tetraoxa-13-azacyclopentadecan-13-yl)-phenyl)-1H-pyrazol-4-yl)-6-diethylamino-3H-xanthen-3-one (16). Rhodol 12b (0.44 g, 0.82 mmol), azacrown ether 15 (0.22 g, 1 mmol), lithium *tert*-butoxide (0.16 g, 2 mmol), and palladium diacetate (20 mg, 0.09 mmol) were placed into a dried Schenk flask. The flask was capped, subsequently degassed several times, and filled with argon. Then a 0.25 M toluene solution of tri-*tert*-butylphosphine (0.3 mL, 0.075 mmol) and 5 mL of dry degassed dioxane were added to the inert atmosphere. The stirred reaction mixture was heated at 90 °C for 24 h. On cooling, the mixture was diluted with CH₂Cl₂ (30 mL) and solid material was filtered off. Solvents were evaporated, and the residue was eluted through the silica column (CH₂Cl₂–CH₃OH 9:1). The fraction consisting of compound 16 was evaporated. The crude product was purified on SEC in THF to give 0.21 g (41%) of the title compound. Mp: 200–201 °C. ¹H NMR (500 MHz, CDCl₃): 8.00 (s, 1H), 7.84 (s, 1H), 7.57 (d, J 9.2 Hz, 2H), 7.52 (d, J 9.2 Hz, 1H), 7.50 (d, J 9.7 Hz, 1H), 6.76 (d, J 9.2 Hz, 2H), 6.66–6.61 (m, 2H), 6.60 (d, J 2.6 Hz, 1H), 6.44 (d, J 1.9 Hz, 1H), 3.80 (t, J 6.2 Hz, 4H), 3.73–3.60 (m, 16H), 3.49 (q, J 7.3 Hz, 4H), 1.27 (t, J 7.1 Hz, 6H). ¹³C NMR (125 MHz, CDCl₃): 159.0, 155.8, 152.2, 147.2, 141.8, 141.0, 130.4, 129.8, 129.1, 128.2, 127.7, 121.2, 115.1, 114.4, 111.8, 110.4, 109.8, 105.3, 96.8, 71.3, 70.3, 70.1, 68.4, 52.7, 45.1, 12.6. HRMS (ESI-TOF): calcd for C₃₆H₄₂N₄O₆ 627.3183 [M + H⁺], found 627.3190. Anal. Calcd for C₃₆H₄₂N₄O₆ (626.74): C, 68.99; H, 6.75; N, 8.94. Found: C, 68.73; H, 6.69; N, 8.83. λ_{abs} (CH₃CN, $\epsilon \times 10^{-3}$): 297 (34), 490 (42), 524 (53) nm.

■ ASSOCIATED CONTENT

📄 Supporting Information

Normalized absorption spectra for dyes 14 and 16, two-photon absorption spectrum of compound 12a in DMSO, as well as ¹H NMR and ¹³C NMR spectra for compounds 4–7, 9, 10, 11a,b, 12a,b, 14, and 16. This material is available free of charge via Internet at <http://pubs.acs.org>.

■ AUTHOR INFORMATION

Corresponding Authors

*E-mail: mireille.blanchard-desce@u-bordeaux1.fr.

*E-mail: dtgryko@icho.edu.pl.

Notes

The authors declare no competing financial interest.

■ ACKNOWLEDGMENTS

This work was funded by the Foundation for Polish Science (TEAM-2009-4/3).

■ REFERENCES

- (1) Gokel, G. W.; Leevy, W. M.; Weber, M. E. *Chem. Rev.* **2004**, *104*, 2723–2750.
- (2) Callan, J. F. A.; de Silva, P.; Magri, D. C. *Tetrahedron.* **2005**, *61*, 8551–8588.
- (3) Kim, H. M.; Choo, H.-J.; Jung, S.-Y.; Ko, Y.-G.; Park, W.-H.; Jeon, S.-J.; Kim, C. H.; Joo, T.; Cho, B. R. *ChemBioChem* **2007**, *8*, 553–559.
- (4) Yao, S.; Ahn, H.-Y.; Wang, X.; Fu, J.; Van Stryland, E. W.; Hagan, D. J.; Belfield, K. D. *J. Org. Chem.* **2010**, *75*, 3965–3974.
- (5) Andrade, C. D.; Yanez, C. O.; Rodriguez, L.; Belfield, K. D. *J. Org. Chem.* **2010**, *75*, 3975–3982.
- (6) Larson, D. R.; Zipfel, W. R.; Williams, R. M.; Clark, S. W.; Bruchez, M. P.; Wise, F. W.; Webb, W. W. *Science* **2003**, *300*, 1434–1437.
- (7) Ventelon, L.; Charier, S.; Moreaux, L.; Mertz, J.; Blanchard-Desce, M. *Angew. Chem., Int. Ed.* **2001**, *40*, 2098–2101.

- (8) Tathavarty, R. K.; Parent, M.; Werts, M. H. V.; Gmouh, S.; Caminade, A.-M.; Moreaux, L.; Charpak, S.; Majoral, J.-P.; Blanchard-Desce, M. *Angew. Chem., Int. Ed.* **2006**, *45*, 4645–4648.
- (9) Pawlicki, M.; Collins, H. A.; Denning, R. G.; Anderson, H. L. *Angew. Chem.* **2009**, *121*, 3292–3316; *Angew. Chem., Int. Ed.* **2009**, *48*, 3244–3266.
- (10) Kim, H. M.; Cho, B. R. *Chem. Commun.* **2009**, 153–164.
- (11) Meier, H. *Angew. Chem.* **2005**, *117*, 2536–2561; *Angew. Chem., Int. Ed.* **2005**, *44*, 2482–2506.
- (12) (a) Sumalekshmy, S.; Fahrni, C. J. *Chem. Mater.* **2011**, *23*, 483–500. (b) Yao, S.; Belfield, K. D. *Eur. J. Org. Chem.* **2012**, *17*, 3199–3217.
- (13) (a) Pond, S. J. K.; Tsutsumi, O.; Rumi, M.; Kwon, O.; Zojer, E.; Bredas, J.-L.; Marder, S. R.; Perry, J. W. *J. Am. Chem. Soc.* **2004**, *126*, 9291–9306. (b) Kim, H. M.; Jeong, M.-Y.; Ahn, H. C.; Jeon, S.-J.; Cho, B. R. *J. Org. Chem.* **2004**, *69*, 5749–5751. (c) Mateeva, N.; Deiab, S.; Archibong, E.; Tasheva, D.; Mochona, B.; Gangapuram, M.; Redda, K. *Int. J. Chem.* **2011**, *3*, 10–17.
- (14) Rumi, M.; Barlow, S.; Wang, J.; Perry, J. W.; Marder, S. R. *Adv. Polym. Sci.* **2008**, *213*, 1–95.
- (15) He, G. S.; Tan, L.-S.; Zheng, Q.; Prasad, P. N. *Chem. Rev.* **2008**, *108*, 1245–1330.
- (16) Kim, H. M.; Cho, B. R. *Acc. Chem. Res.* **2009**, *42*, 863–872.
- (17) Albota, M.; Beljonne, D.; Brédas, J.-L.; Ehrlich, J. E.; Fu, J.-Y.; Heikal, A. A.; Hess, S. E.; Kogej, T.; Levin, M. D.; Marder, S. R.; McCord-Maughon, D.; Perry, J. W.; Röckel, H.; Rumi, M.; Subramaniam, G.; Webb, W. W.; Wu, X.-L.; Xu, C. *Science* **1998**, *281*, 1653–1656.
- (18) Chung, S.-J.; Rumi, M.; Alain, V.; Barlow, S.; Perry, J. W.; Marder, S. R. *J. Am. Chem. Soc.* **2005**, *127*, 10844–10845.
- (19) Mongin, O.; Porrès, L.; Charlot, M.; Katan, C.; Blanchard-Desce, M. *Chem.—Eur. J.* **2007**, *13*, 1481–1498.
- (20) Zheng, S.; Beverina, L.; Barlow, S.; Zojer, E.; Fu, J.; Padilha, L. A.; Fink, C.; Kwon, O.; Yi, Y.; Shuai, Z.; Van Stryland, E. W.; Hagan, D. J.; Brédas, J.-L.; Marder, S. R. *Chem. Commun.* **2007**, 1372–1374.
- (21) Zheng, S.; Leclercq, A.; Fu, J.; Beverina, L.; Padilha, L. A.; Zojer, E.; Schmidt, K.; Barlow, S.; Luo, J.; Jiang, S.-H.; Jen, A. K.-Y.; Yi, Y.; Shuai, Z.; Van Stryland, E. W.; Hagan, D. J.; Brédas, J.-L.; Marder, S. R. *Chem. Mater.* **2007**, *19*, 432–442.
- (22) Belfield, K. D.; Bondar, M. V.; Yanez, C. O.; Hernandez, F. E.; Przhonska, O. V. *J. Mater. Chem.* **2009**, *19*, 7498–7502.
- (23) Barzoukas, M.; Blanchard-Desce, M. *J. Chem. Phys.* **2000**, *113*, 3951–3959.
- (24) (a) Ventelon, L.; Moreaux, L.; Mertz, J.; Blanchard-Desce, M. *Chem. Commun.* **1999**, 2055–2056. (b) Mongin, O.; Porrès, L.; Moreaux, L.; Mertz, J.; Blanchard-Desce, M. *Org. Lett.* **2002**, *4*, 719–722.
- (25) Le Droumaguet, C.; Sourdon, A.; Genin, E.; Mongin, O.; Blanchard-Desce, M. *Chem. Asian J.* **2013**, DOI: 10.1002/asia.201300735.
- (26) (a) Kim, H. M.; Cho, B. R. *Chem.—Asian J.* **2011**, *6*, 58–69. (b) Blanchard-Desce, M. C. R. *Physique* **2002**, *3*, 439–448. (c) Ha-Thi, M.-H.; Penhoat, M.; Drouin, D.; Blanchard-Desce, M.; Michelet, V.; Leray, I. *Chem.—Eur. J.* **2008**, *14*, 5941–5950.
- (27) Ahn, H.-Y.; Fairfull-Smith, K. E.; Morrow, B. J.; Lussini, V.; Kim, B.; Bondar, M. V.; Bottle, S. E.; Belfield, K. D. *J. Am. Chem. Soc.* **2012**, *134*, 4721–4730.
- (28) Seo, E. W.; Han, J. H.; Heo, C. H.; Shin, J. H.; Kim, H. M.; Cho, B. R. *Chem.—Eur. J.* **2012**, *18*, 12388–12394.
- (29) Heo, C. H.; Park, S. K.; Lim, C. S.; Park, M. K.; Kim, H. J.; Kim, H. M.; Cho, B. R. *Chem.—Eur. J.* **2012**, *18*, 15246–15249.
- (30) Dong, X.; Han, J. H.; Heo, C. H.; Kim, H. M.; Liu, Z.; Cho, B. R. *Anal. Chem.* **2012**, *84*, 8110–8113.
- (31) Das, S. K.; Lim, C. S.; Yang, S. Y.; Han, J. H.; Cho, B. R. *Chem. Commun.* **2012**, *48*, 8395–8397.
- (32) Bae, S. K.; Heo, C. H.; Choi, D. J.; Sen, D.; Joe, E.-H.; Cho, B. R.; Kim, H. M. *J. Am. Chem. Soc.* **2013**, *135*, 9915–9923.
- (33) Morales, A. R.; Frazer, A.; Woodward, A. W.; Ahn-White, H.-Y.; Fonari, A.; Tongwa, P.; Timofeeva, T.; Belfield, K. D. *J. Org. Chem.* **2013**, *78*, 1014–1025.
- (34) Morales, A. R.; Yanez, C. O.; Zhang, Y.; Wang, X.; Biswas, S.; Urakami, T.; Komatsu, M.; Belfield, K. D. *Biomaterials* **2012**, *33*, 8477–8485.
- (35) (a) Ushakov, E. N.; Alfimov, M. V.; Gromov, S. P. *Russ. Chem. Rev.* **2008**, *77*, 39–58. (b) Kim, K.; Choi, S. H.; Jeon, J.; Lee, H.; Huh, J. O.; Yoo, J.; Kim, J. T.; Lee, C.-H.; Lee, Y. S.; Churchill, D. G. *Inorg. Chem.* **2011**, *50*, 5351–5360. (c) Kim, K.; Jo, C.; Easwaramoorthi, S.; Sung, J.; Kim, D. H.; Churchill, D. G. *Inorg. Chem.* **2010**, *49*, 4881–4894. (d) Kim, K.; Ha, Y.; Kaufman, L.; Churchill, D. G. *Inorg. Chem.* **2012**, *51*, 928–938.
- (36) Tsukanov, A. V.; Dubonosov, A. D.; Bren, V. A.; Minkin, V. I. *Chem. Heterocycl. Compd.* **2008**, *44*, 899–923.
- (37) Daehne, S.; Resch-Genger, U.; Wolfbeis, O. S. *Near-Infrared Dyes for High Technology Applications*; Kluwer Academic Publishers: London, 1998.
- (38) Raue, R.; Harnisch, H.; Drexhage, K. H. *Heterocycles* **1984**, *21*, 167–190.
- (39) Zollinger, H. *Color Chemistry*, 3rd ed.; Wiley-VCH: Weinheim, 2003.
- (40) Shirinian, V. Z.; Shimkin, A. A. *Top. Heterocycl. Chem.* **2008**, *14*, 75–105.
- (41) Kulinich, A. V.; Ishchenko, A. A. *Russ. Chem. Rev.* **2009**, *78*, 141–164.
- (42) Genin, E.; Hugues, V.; Clermont, G.; Herbivo, C.; Castro, M. C. R.; Comel, A.; Raposo, M. M. M.; Blanchard-Desce, M. *Photochem. Photobiol. Sci.* **2012**, *11*, 1756–1766.
- (43) Poronik, Y. M.; Hugues, V.; Blanchard-Desce, M.; Gryko, D. T. *Chem.—Eur. J.* **2012**, *18*, 9258–9266.
- (44) Svetlichnyi, V. A.; Ishchenko, A. A.; Vaitulevich, E. A.; Derevyanko, N. A.; Kulinich, A. V. *Opt. Commun.* **2008**, *281*, 6072–6079.
- (45) Gerasov, A. O.; Shandura, M. P.; Kovtun, Y. P. *Dyes Pigm.* **2008**, *77*, 598–607.
- (46) Padilha, L. A.; Webster, S.; Przhonska, O. V.; Hu, H.; Peceli, D.; Rosch, J. L.; Bondar, M. V.; Gerasov, A. O.; Kovtun, Y. P.; Shandura, M. P.; Kachkovski, A. D.; Hagan, D. J.; Van Stryland, E. W. *J. Mater. Chem.* **2009**, *19*, 7503–7513.
- (47) Webster, S.; Fu, J.; Padilha, L. A.; Przhonska, O. V.; Hagan, D. J.; Van Stryland, E. W.; Bondar, M. V.; Slominsky, Y. L.; Kachkovski, A. D. *Chem. Phys.* **2008**, *348*, 143–151.
- (48) Sauters, R. R.; Husain, S. N.; Piechowski, A. P.; Bird, G. R. *Dyes Pigm.* **1987**, *8*, 35–53.
- (49) Burdette, S. C.; Lippard, S. J. *Inorg. Chem.* **2002**, *41*, 6816–6823.
- (50) Tomat, E.; Lippard, S. J. *Inorg. Chem.* **2010**, *49*, 9113–9115.
- (51) Kamiya, M.; Asanuma, D.; Kuranaga, E.; Takeishi, A.; Sakabe, M.; Miura, M.; Nagano, T.; Urano, Y. *J. Am. Chem. Soc.* **2011**, *133*, 12960–12963.
- (52) Clark, M. A.; Duffy, K.; Tibrewala, J.; Lippard, S. J. *Org. Lett.* **2003**, *5*, 2051–2054.
- (53) (a) Peng, T.; Yang, D. *Org. Lett.* **2010**, *12*, 496–499. (b) Peng, T.; Yang, D. *Org. Lett.* **2010**, *12*, 4932–4935.
- (54) Azizian, F.; Field, A. J.; Griffiths, J.; Heron, B. M. *Dyes Pigm.* **2012**, *92*, 524–530.
- (55) Wen, H.; Huang, Q.; Yang, X.-F.; Li, H. *Chem. Commun.* **2013**, *49*, 4956–4958.
- (56) Kamino, S.; Ichikawa, H.; Wada, S.; Horio, Y.; Usami, Y.; Yamaguchi, T. *Bioorg. Med. Chem. Lett.* **2008**, *18*, 4380–4384.
- (57) Komatsu, H.; Harada, H.; Tanabe, K.; Hiraoka, M.; Nishimoto, S. *Med. Chem. Commun.* **2010**, *1*, 50–53.
- (58) Lv, X.; Liu, J.; Liu, Y.; Zhao, Y.; Chen, M.; Wang, P.; Guo, W. *Sensors Actuators B* **2011**, *158*, 405–410.
- (59) Lee, L. G.; Berry, G. M.; Chen, C.-H. *Cytometry* **1989**, *10*, 151–164.
- (60) Johnson, I.; Spence, M. T. Z. *Molecular Probes Handbook, A Guide to Fluorescent Probes and Labeling Technologies*, 11th ed.; Molecular Probes: Eugene, OR, 2010.

- (61) Gokel, G. W. *Crown Ethers and Cryptands*; Royal Society of Chemistry: London, 1994.
- (62) Fabrizzi, L.; Poggi, A. *Chem. Soc. Rev.* **1995**, 197–202.
- (63) Poronik, Y. M.; Shandura, M. P.; Kovtun, Y. P. *Dyes Pigm.* **2007**, 72, 199.
- (64) Mao, F.; Leung, Y.-Y.; Cheung, C.-Y.; Hoover, H.-E. Heterocycle-Substituted Xanyjene Dyes. WO2011068569, June 9, 2011.
- (65) Shandura, M. P.; Poronik, Y. M.; Kovtun, Yu. P. *Dyes Pigm.* **2007**, 73, 25–30.
- (66) Sakamoto, H.; Kimura, K.; Koseki, Y.; Matsuo, M.; Shono, T. *J. Org. Chem.* **1986**, 51, 4974–4979.
- (67) Gatto, V. J.; Gokel, G. W. *J. Am. Chem. Soc.* **1984**, 106, 8240–8244.
- (68) Gatto, V. J.; Arnold, K. A.; Viscariello, A. M.; Miller, S. R.; Gokel, G. W. *Tetrahedron Lett.* **1986**, 27, 327–330.
- (69) Zhang, X.-X.; Buchwald, S. L. *J. Org. Chem.* **2000**, 65, 8027–8031.
- (70) Urgaonkar, S.; Verkade, J. G. *Tetrahedron* **2004**, 60, 11837–11842.
- (71) Witulski, B.; Weber, M.; Bergstrasser, U.; Desvergne, J.-P.; Bassani, D. M.; Bouas-Laurent, H. *Org. Lett.* **2001**, 3, 1467–1470.
- (72) Sazonov, P. K.; Artamkina, G. A.; Beletskaya, I. P.; Russ.. *J. Org. Chem.* **2006**, 42, 438–447.
- (73) Mikhailitsyna, E. A.; Tyurin, V. S.; Zamyatskov, I. A.; Beletskaya, I. P.; Khrustalev, V. N. *Dalton Trans.* **2012**, 41, 7624–7636.
- (74) Kobelev, S. M.; Averin, A. D.; Beletskaya, I. P.; Buryak, A. K.; Denat, F.; Guilard, R. *Tetrahedron Lett.* **2012**, 53, 210–213.
- (75) Brandel, J.; Sairenji, M.; Ichikawa, K.; Nabeshima, T. *Chem. Commun.* **2010**, 46, 3958–3960.
- (76) López Arbeloa, F.; Ruiz Ojeda, P.; López Arbeloa, I. J. *Luminesc.* **1989**, 44, 105–112.
- (77) Mustorph, H.; Reiner, K.; Mistol, J.; Ernst, S.; Keil, D.; Hennig, L. *Chem. Phys. Chem.* **2009**, 10, 835–840.
- (78) Mustorph, H.; Mistol, J.; Senns, B.; Keil, D.; Findeisen, M.; Hennig, L. *Angew. Chem., Int. Ed.* **2009**, 48, 8773–8775.
- (79) Kim, M. K.; Lim, C. S.; Hong, J. T.; Han, J. H.; Jang, H.-Y.; Kim, H. M.; Cho, B. R. *Angew. Chem., Int. Ed.* **2010**, 49, 364–367.
- (80) Kim, H. J.; Han, J. H.; Kim, M. K.; Lim, C. S.; Kim, H. M.; Cho, B. R. *Angew. Chem., Int. Ed.* **2010**, 49, 6786–6789.
- (81) (a) Albota, M. A.; Xu, C.; Webb, W. W. *Appl. Opt.* **1998**, 37, 7352–7356. (b) Xu, C.; Webb, W. W. *J. Opt. Soc. Am. B* **1996**, 13, 481–491.
- (82) Werts, M. H. V.; Nerambourg, N.; Pélégry, D.; Le Grand, Y.; Blanchard-Desce, M. *Photochem. Photobiol. Sci.* **2005**, 4, 531–538.
- (83) Katan, C.; Tretiak, S.; Werts, M. H. V.; Bain, A. J.; Marsh, R. J.; Leoczek, N.; Nicolaou, N.; Badaeva, E.; Mongin, O.; Blanchard-Desce, M. *J. Phys. Chem. B* **2007**, 111, 9468–9483.